PDZRhoGEF and myosin II localize RhoA activity to the back of polarizing neutrophil-like cells

Kit Wong,[1] Alexandra Van Keymeulen,[2] and Henry R. Bourne[1]

[1]Department of Cellular and Molecular Pharmacology, University of California, San Francisco, San Francisco, CA 94158
[2]Interdisciplinary Research in Human and Molecular Biology Institute (IRIBHM), Faculty of Medicine, Université Libre de Bruxelles (ULB), 1070 Brussels, Belgium

Chemoattractants such as formyl-Met-Leu-Phe (fMLP) induce neutrophils to polarize by triggering divergent pathways that promote formation of a protrusive front and contracting back and sides. RhoA, a Rho GTPase, stimulates assembly of actomyosin contractile complexes at the sides and back. We show here, in differentiated HL60 cells, that PDZRhoGEF (PRG), a guanine nucleotide exchange factor (GEF) for RhoA, mediates RhoA-dependent responses and determines their spatial distribution. As with RNAi knock-down of PRG, a GEF-deleted PRG mutant blocks fMLP-dependent RhoA activation and causes neutrophils to exhibit multiple fronts and long tails. Similarly, inhibition of RhoA, a Rho-dependent protein kinase (ROCK), or myosin II produces the same morphologies. PRG inhibition reduces or mislocalizes monophosphorylated myosin light chains in fMLP-stimulated cells, and myosin II ATPase inhibition reciprocally disrupts normal localization of PRG. We propose a cooperative reinforcing mechanism at the back of cells, in which PRG, RhoA, ROCK, myosin II, and actomyosin spatially cooperate to consolidate attractant-induced contractility and ensure robust cell polarity.

Introduction

Cell polarity is essential for many cells of metazoans, as exemplified by the axons and dendrites of developing neurons, the apical and basolateral domains of epithelial cells, and the morphologically distinct front and back of migrating cells, such as chemotaxing neutrophils. The RhoGTPases RhoA, Rac, and Cdc42 regulate cell polarity (Fukata et al., 2003; Raftopoulou and Hall, 2004) and are activated under spatial and temporal control by more than 70 guanine nucleotide exchange factors (GEFs) of the Rho GEF family (Rossman et al., 2005). To understand regulation of cell polarity, it is necessary to identify the relevant Rho GEFs, their target Rho GTPases, and their location of activation.

In differentiated HL60 (dHL60) cells, a neutrophil-like cell line, stimulation with a chemoattractant, such as the tripeptide formyl-Met-Leu-Phe (fMLP), induces cell polarity (Hauert et al., 2002). Symmetry is broken by activating divergent signaling pathways for controlling the formation of front and back (Xu et al., 2003; Wong et al., 2006). Signals downstream of Gi, phospatidylinositol-3′-kinase (PI3K), Rac, and F-actin participate in positive feedback loops that mediate protrusive actin assembly at the front (Niggli, 2000; Wang et al., 2002; Weiner et al., 2002). At the back, G12 and 13 promote activation of RhoA and its downstream mediators, a Rho-dependent kinase (ROCK) and myosin II, resulting in formation of contractile actomyosin complexes (Xu et al., 2003).

Together, these divergent pathways constitute a self-organizing mechanism that allows dHL60 cells to polarize without a spatial cue—that is, after stimulation with a spatially uniform concentration of chemoattractant (Shields and Haston, 1985; Xu et al., 2003; Wong et al., 2006). After uniform stimulation, frontness- and backness-promoting activities initially overlap at the cell periphery but then segregate to form a single front and a single back (Xu et al., 2003; Wong et al., 2006). Cells lacking phospatidylinositol-3,4,5-tris-phosphate (PIP3) or Cdc42 signaling exhibit unstable polarity, characterized by transient but multiple fronts and backs (Van Keymeulen et al., 2006). We proposed that signals for the front, PIP3 and Cdc42, enhance both front and back signals (Van Keymeulen et al., 2006), perhaps by locally regulating Rac GEFs in the pseudopod at the front while increasing activities of RhoA GEFs at longer range to suppress formation of lateral pseudopods at the back and sides.

Recent studies demonstrated that PIX-α and DOCK2, GEFs for Cdc42 and Rac2, respectively, are recruited to the plasma membrane by PIP3 in response to chemoattractant stimulation (Li et al., 2003; Kunisaki et al., 2006). Mouse neutrophils lacking PIX-α, similar to those lacking PI3Kγ (Hirsch et al., 2000;

Correspondence to Henry R. Bourne: bourne@cmp.ucsf.edu

Abbreviations used in this paper: CA, constitutively active; dHL60, differentiated HL60; DN, dominant-negative; fMLP, formyl-Met-Leu-Phe; FRET, fluorescence resonance energy transfer; GEF, guanine nucleotide exchange factor; KD, knock-down; PRG, PDZRhoGEF; PIP3, phospatidylinositol-3,4,5-tris-phosphate; PI3K, phospatidylinositol-3′-kinase; ROCK, Rho-dependent kinase; shRNA, short hairpin RNA.

The online version of this article contains supplemental material.

The Journal of Cell Biology, Vol. 179, No. 6, December 17, 2007 1141–1148
http://www.jcb.org/cgi/doi/10.1083/jcb.200706167

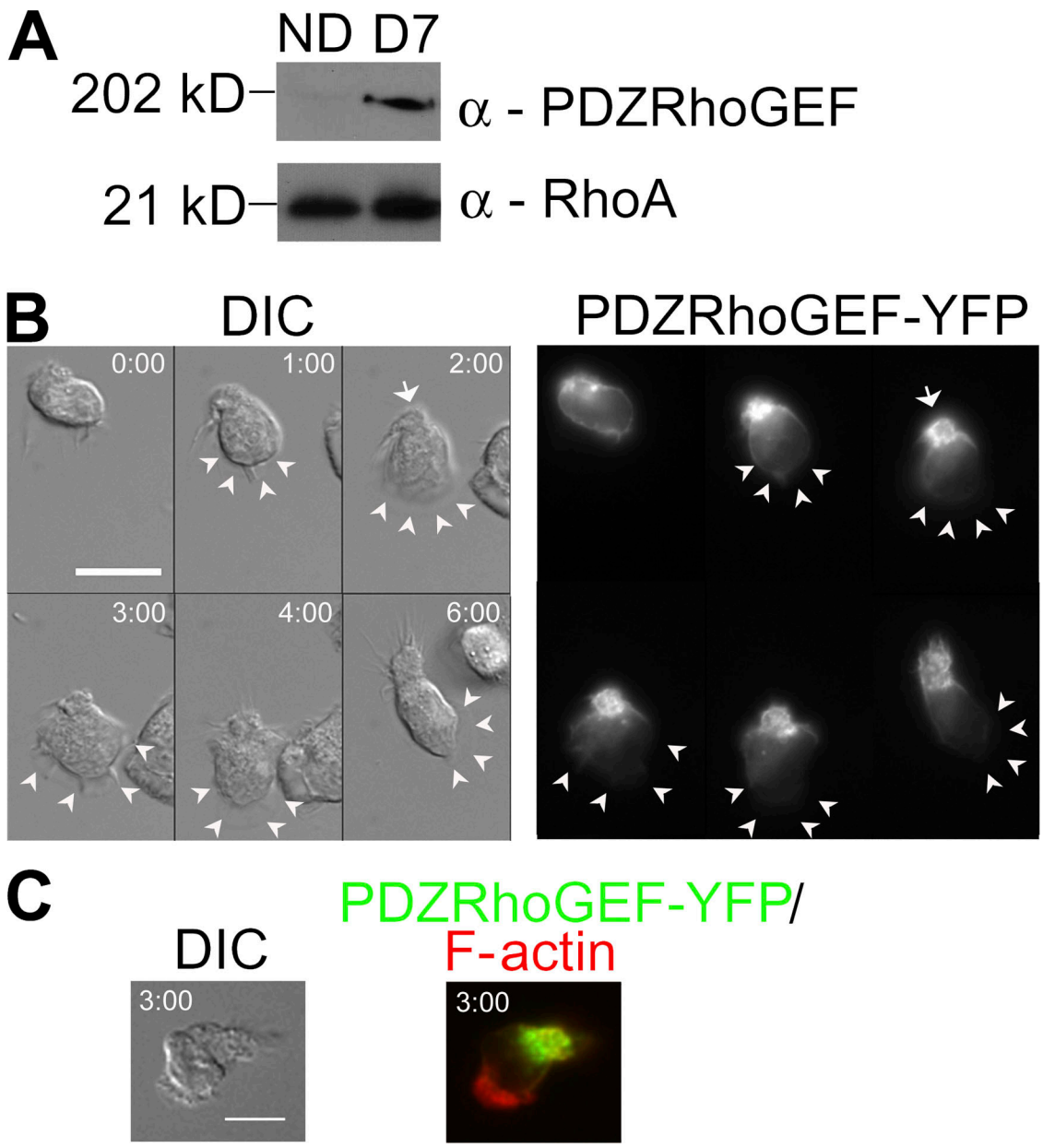

Figure 1. **Expression and localization of PRG in dHL60 cells.** (A) Lysates from nondifferentiated dHL60 cells (ND) or cells differentiated for 7 d (D7) were immunoblotted for PRG protein. RhoA was used as a loading control. (B) DIC and fluorescent time-lapse images of a live dHL60 cell transfected with PRG-YFP. Time indicates elapsed time after uniform addition of 100 nM fMLP at 0:00. (C) DIC and fluorescent images of a representative polarized cell showing PRG-YFP (green) and actin (red). Cells transfected with PRG-YFP were stimulated with 100 nM fMLP for 3 min, fixed, and stained for F-actin. Arrowheads outline pseudopod; arrow depicts the cell's back. Bar = 10 μm.

Li et al., 2000; Hannigan et al., 2002), exhibit defective chemotaxis in chemoattractant gradients (Li et al., 2003). DOCK2-deficient mouse neutrophils fail to accumulate F-actin and PIP3 at the leading edge and show abnormal polarity and migration (Kunisaki et al., 2006).

Lsc (also known as p115RhoGEF) has been reported (Francis et al., 2006) to activate neutrophil RhoA in response to attractant stimulation and is required for integrin-dependent adhesion. Lsc-deficient mouse neutrophils fail to polarize with a single pseudopod and show reduced directionality. Lsc localization at the leading edge (Francis et al., 2006), however, does not mimic the distribution of active RhoA (Xu et al., 2003; Wong et al., 2006), suggesting that other GEFs participate in regulation of RhoA at the sides and back. PDZRhoGEF (PRG), which contains a G12/13-coupled RGS domain and a GEF domain known to activate RhoA (Fukuhara et al., 1999; Rumenapp et al., 1999), represents an appealing candidate regulator for RhoA-dependent backness. PRG plays essential roles in polarity of neurons and ciliated epithelia (Swiercz et al., 2002; Basile et al., 2004; Longhurst et al., 2006; Panizzi et al., 2007). Its *Drosophila* orthologue in S2 cells, DRhoGEF2, localizes to plus ends of microtubules for delivery to the cell periphery (Rogers et al., 2004). In the presence of active Concertina, a G12/13 orthologue, DRhoGEF2 is released from microtubules to activate RhoA at the cell membrane,

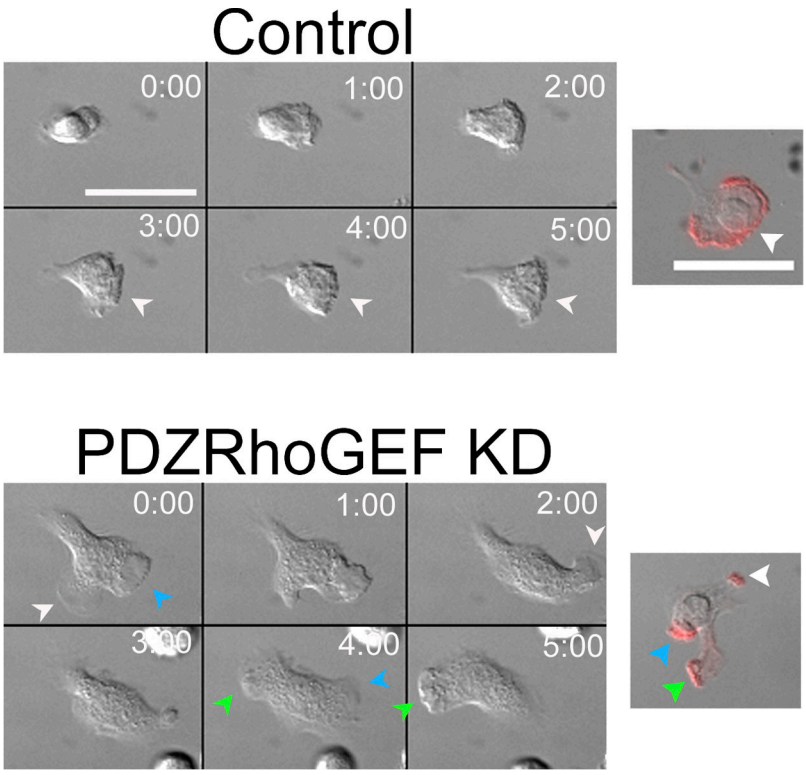

Figure 2. **PRG depletion disrupts fMLP-induced polarity.** DIC time-lapse images of dHL60 cells expressing luciferase-targeted control or PRG-targeted shRNA. (Right) DIC and fluorescent overlays of control and PRG KD cells processed as in Fig. 1 C. Time indicates elapsed time after uniform stimulation with 100 nM fMLP. Different arrowhead colors indicate separate pseudopod. Bars = 10 μm.

thereby generating actomyosin-dependent contraction (Rogers et al., 2004). Here, we show that PRG mediates activation of G12/13-RhoA-dependent backness and is necessary for polarization of dHL60 cells. We describe a cooperative mechanism in which back-promoting signals and the resulting contraction of actomyosin spatially confine one another, consolidating backness signals to ensure robust cell polarity.

Results and discussion

Expression and localization of PRG

Peripheral blood leukocytes contain PRG mRNA (Fukuhara et al., 1999), and PRG protein is expressed much more strongly in differentiated HL60 cells than undifferentiated cells (Fig. 1 A). This differentiation-induced expression resembles that of other polarity components, such as Hem1 (unpublished data), and probably contributes to neutrophil-like properties of differentiated HL60 cells.

PRG's spatial distribution during polarization shows that it is present in the right place at the right time to function as a potential regulator of RhoA during fMLP-induced polarization. The PRG-specific antibody failed to detect specific immunofluorescence staining. To determine the localization of PRG, we transiently expressed PRG-YFP. High expression of PRG-YFP, assessed by degree of cell fluorescence, correlated with a rounded cell morphology (unpublished data) similar to that induced by dominant-positive RhoA (Xu et al., 2003). To obtain low expression of PRG, we used cells at 3 h post-transfection or expressed PRG-YFP under a leaky tetracycline-inducible promoter in the absence of tetracycline. Time-lapse fluorescent images show that PRG-YFP is partly cytosolic but is located mostly at the cell periphery. fMLP causes PRG-YFP, localized uniformly at the periphery of resting cells, to shift to a back-concentrated distribution in polarized cells (86% of cells examined, $n = 42$; Fig. 1, B and C). PRG is markedly excluded from the actin-rich front and partially colocalizes with actin at the back (Fig. 1 C). The increased actin at the back probably reflects local elevation of actomyosin complexes caused by increased RhoA activity.

PRG is necessary for fMLP-induced polarity and RhoA activation

To study PRG's function in polarization in dHL60 cells, we used a lentiviral-mediated short hairpin RNA (shRNA) to knock down its expression. PRG protein is dramatically reduced in knockdown (KD) cells (Fig. S1 A, available at http://www.jcb.org/cgi/content/full/jcb.200706167/DC1).

PRG is required for fMLP-induced polarity in dHL60 cells. In contrast to control cells, which polarize with a single actin-rich pseudopod and a single retracting back (Fig. 2; Fig. S1 B), PRG KD cells often show multiple pseudopods or long tails (Fig. 2; S1 B) and migrate with reduced speed and persistence (Fig. S1 C). Inactivation of RhoA, ROCK, or myosin II ATPase in dHL60 cells induced similar morphologies (Xu et al., 2003). Re-introduction of a myc-tagged rat PRG orthologue (Myc-rPRG; identified by RFP coexpression) rescues the KD phenotype (Fig. S1, B–D), suggesting that PRG mediates the fMLP-induced activation of myosin II by activating RhoA.

PRG's DH-PH domain is required for its localization to the back and function during polarization. Expression of a DH-PH deleted mutant (1–735 aa; Fig. S2 A, available at http://www.jcb.org/cgi/content/full/jcb.200706167/DC1), which has been shown to lack GEF activity in other cell types (Fukuhara et al., 1999;

Driessens et al., 2002; Banerjee and Wedegaertner, 2004), causes a phenotype similar to that induced by shRNA-mediated KD of PRG (7/8 cells examined; Fig. S2 B). In contrast to the back-enriched localization of wild-type PRG-YFP, this YFP-tagged mutant (1–735-YFP) localizes to actin-rich pseudopods, which are often multiple (Fig. S2, B and B′).

Unlike the 1–735-YFP construct, expression of N-terminal deletion mutants lacking the PDZ or the PDZ plus the RGS (128–1522 or 435–1522; Fig. S2 A) domains does not affect formation of polarity, but does destabilize polarity in some cells: the region occupied by a front becomes a back and vice versa, resulting in reversal of polarity (6/11 cells for 128–1522, 4/10 cells for 435–1522; example in Fig. S2 C). In contrast to the stable polarity maintained throughout the course of imaging in cells expressing wild-type PRG-YFP (7/8 cells; Fig. 1 B), cells expressing either of these N-terminal deletion mutants accumulate mutant PRG-YFP at both the front and the back (Fig. S2, C and C′; arrowheads and arrows). These results suggest that normally the PDZ domain, in the presence of DH-PH domain, keeps the protein at the back. Therefore, restrictive localization of PRG is necessary to establish and maintain dHL60 cell polarity in response to fMLP, probably by regulating the RhoA-dependent back-promoting pathway.

PRG is necessary for fMLP to induce activation of RhoA, as documented by an assay (Niggli, 2003) that assesses association of RhoA with the particulate fraction of cells previously exposed to fMLP. As previously reported, fMLP increases RhoA in the particulate fraction of extracts from neutrophils or dHL60 cells (Niggli, 2003; Van Keymeulen et al., 2006). The attractant fails to do so, however, in PRG KD cells (Fig. 3 A). Similarly, a fluorescence resonance energy transfer (FRET)–based assay for measuring RhoA activity (Wong et al., 2006) shows that in cells coexpressing the RhoA biosensor and a myc-tagged 1–735 PRG (Myc-1–735), fMLP fails to increase RhoA FRET as previously reported in control cells (Wong et al., 2006; unpublished data).

To further characterize the role of PRG, we assessed the localization of monophosphorylated myosin light chain 2 (p-MLC2). Instead of the typical sides-and-back localization seen in fMLP-stimulated control cells, KD cells deficient in endogenous PRG exhibit multiple heads with reduced or mislocalized p-MLC2 (Fig. 3 B). Re-introduction of Myc-rPRG restores the cells' ability to polarize, making a single actin-rich front (Fig. 3 B, green) and a single back enriched in p-MLC2 and Myc-rPRG (Fig. 3 B, red and blue panels). The increased actin staining at the back is similar to the effect of expressing PRG-YFP in wild-type cells (Fig. 1 C). Together, these results indicate that PRG consolidates the front and back by regulating the RhoA-dependent back-promoting pathway.

Similarly, dHL60 cells expressing Myc-1-735 show reduced or mislocalized staining of p-MLC2 that does not overlap with that of Myc-1–735 (Fig. S2 D). Like 1–735-YFP, Myc-1–735 localizes to ruffles. Typical morphologies and their relative frequencies are shown in Fig. S2 A. The reciprocal distribution patterns of p-MLC2 and Myc-1–735 suggest that Myc-1–735 PRG acts by sequestering binding partners that normally interact with endogenous PRG to localize it at the back. One such partner could be G12/13, which may be sequestered by the RGS domain of Myc-1–735 PRG. Alternatively, the PDZ domain in the 1–735 construct might—as reported for rat PRG (Longhurst et al., 2006)—interact with type I PDZ ligands and light chains of microtubule-associated protein 1. In either case, this result implies that PRG in normal cells acts locally to activate RhoA and its downstream pathway, and—reciprocally—that the local "backness" environment created by its GEF activity is necessary for its localization.

We note, however, that a subpopulation of PRG KD cells with multiple leading edges rich in F-actin still exhibit increased accumulation of p-MLC2 at a single site (Fig. 3 B). Because the level of p-MLC2 in KD cells is similar to that of controls, as assayed by immunoblots (unpublished data), it is likely that PRG normally regulates localization rather than the total amount of MLC2 phosphorylation. Alternatively, cell-to-cell variation in expression of PRG shRNA may fail to deplete PRG efficiently in some cells. Myosin II could be activated by other mechanisms as well, involving RhoA GEFs such as Lsc (Francis et al., 2006) as well as RhoA-independent pathways.

G12/13 and myosin II spatially regulate PRG

To ask whether PRG mediates signal transmission between G12/13 and RhoA in response to fMLP, we coexpressed dominant-negative (DN) or constitutively active (CA) mutants of G12/13 together with PRG-YFP in dHL60 cells and assessed localization of PRG-YFP. As previously reported (Xu et al., 2003), cells expressing DN G12 and G13 form multiple leading edges (Fig. 4 A, arrowheads). Moreover, G12/13 regulates the spatial distribution of PRG. Instead of localizing to the cell periphery at the back as in control cells (Fig. 4 A), punctate clusters of PRG distribute throughout cells coexpressing DN G12 and G13, especially around the nucleus (Fig. 4 A). On the other hand, expression of CA G12 and G13 or RhoA (unpublished data) causes cells to round up, with PRG-YFP localized around the entire periphery (Fig. 4 A).

To determine whether myosin II, a downstream target of the G12/13-RhoA pathway, is involved in regulating PRG, we inhibited its ATPase activity with blebbistatin. As previously shown, blebbistatin causes fMLP-stimulated cells to make multiple leading edges or a long tail (Xu et al., 2003). Just as in cells expressing DN G12/13, PRG-YFP in blebbistatin-treated cells localizes in clusters around the nucleus (Fig. 4 A). Inhibiting ROCK with Y-27632 (Narumiya et al., 2000) causes the same phenotype (unpublished data), in keeping with the notion that ROCK acts upstream of myosin II (Xu et al., 2003). These results suggest that localization of PRG depends on myosin II activity. The observed distribution is not due to background fluorescence from blebbistatin; comparing blebbistatin-treated nontransfected cells with transfected cells revealed no noticeable signal in the nontransfected population (Fig. S3, available at http://www. jcb.org/cgi/content/full/jcb.200706167/DC1).

Although myosin II helps to localize PRG, and vice versa, the underlying biochemical mechanisms remain unknown. Backness signals could spatially regulate PRG by somehow directing the transport of PRG-containing vesicles, as suggested by the Golgi-like perinuclear punctate distribution of PRG-YFP in cells disrupted for RhoA-dependent backness signals (Fig. 4 A). Indeed, nonmuscle myosin II is known to be important for the

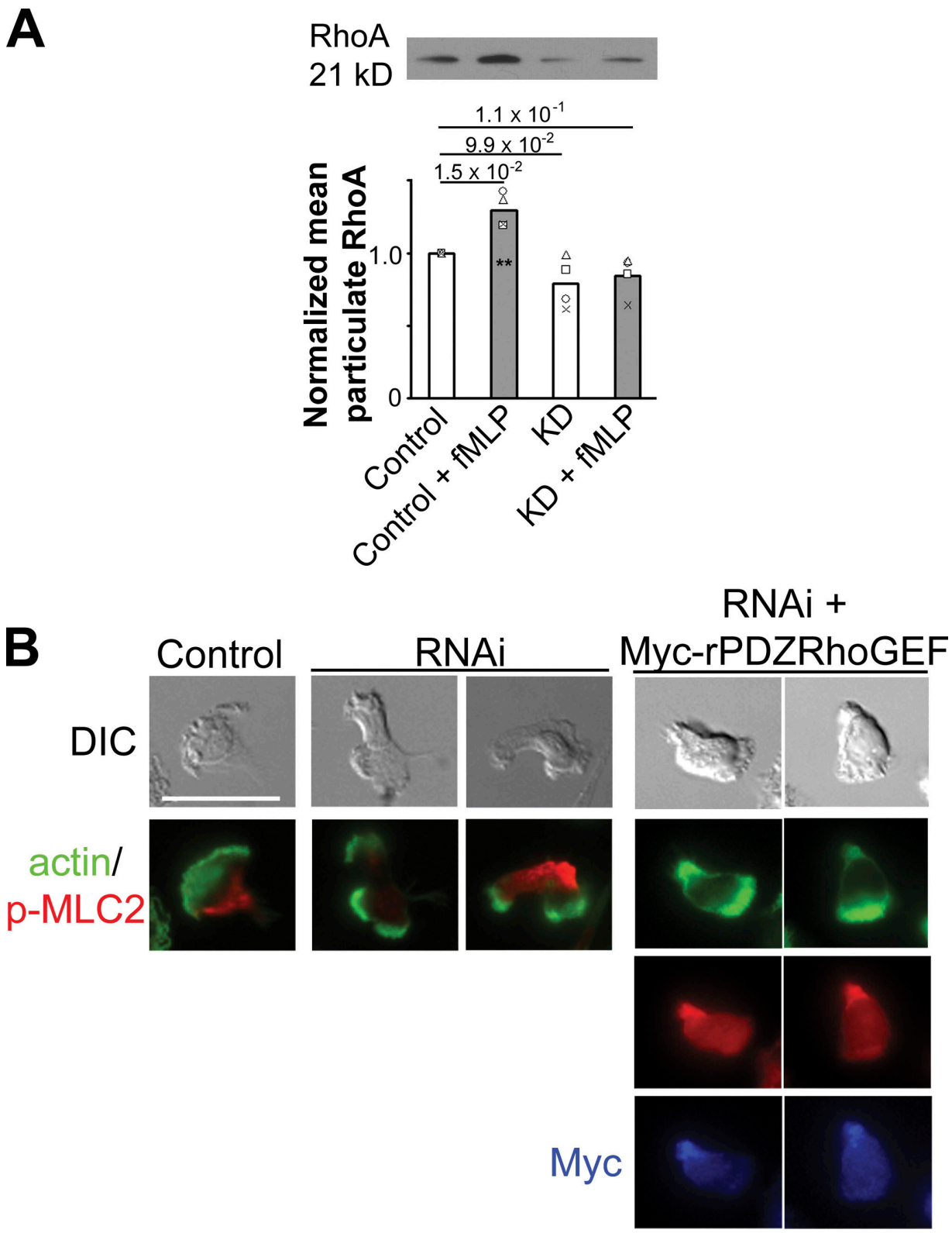

Figure 3. **PRG mediates fMLP-induced RhoA activation and consolidation of front and back.** (A) fMLP-induced membrane association of RhoA. Control or KD cells were stimulated with or without fMLP (100 nM, 1 min) as indicated. RhoA associated with the particulate fraction of cell extracts was assessed as described. A representative immunoblot and quantification of immunoblotted bands are shown. For each immunoblot, background signal was subtracted and the level of RhoA normalized to that of transferrin receptor in the particulate fraction; all values were further normalized to the signal detected in the unstimulated control, set at 1.0. Bar represents the average of four independent experiments, with different symbols representing the actual values. P values are shown. **, $P \leq 0.05$. (B) DIC and fluorescent images of representative cells expressing control or PRG-targeted shRNA with or without a Myc-tagged rat PRG processed as in Fig. 1 C and stained for actin (green), p-MLC2 (red), and Myc (blue). Bars = 10 μm.

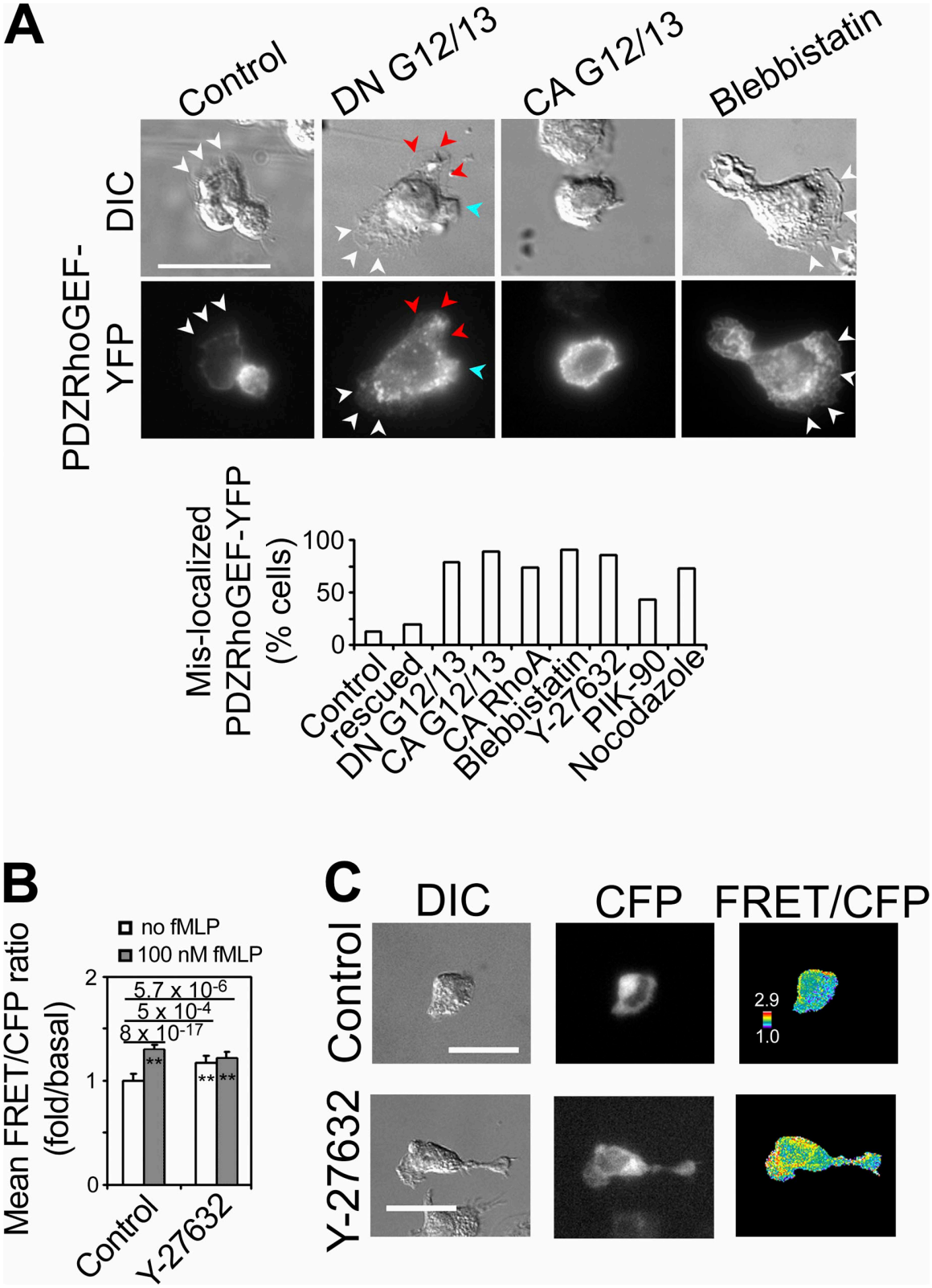

Figure 4. **Spatial distribution of PRG depends on G12/13 and myosin II.** (A) dHL60 cells transiently transfected with PRG-YFP alone, or together with DN or CA G12 and G13 were stimulated with 100 nM fMLP, fixed, and imaged. Representative DIC and fluorescent images of each group are shown. Cells expressing PRG-YFP alone with or without 45 min pretreatment with 100 μM blebbistatin were processed and imaged as above. Percent of cells with mislocalized PRG-YFP was plotted for control (n = 60), KD cells expressing rat PRG (rescued; n = 36), cells coexpressing DN G12/13 (n = 33), CA G12/13 (n = 28), or CA RhoA (n = 31) and cells treated for 45 min with 100 μM blebbistatin (n = 46), 10 μM Y-27632 (n = 29), 1 μM PIK-90 (n = 37), or 25 μM nocodazole (n = 47). (B) Quantification of mean FRET/CFP ratio in RhoA biosensor cells treated with or without Y-27632 (10 μM, 45 min), stimulated and processed as above. Mean FRET/CFP ratios ± SEM (error bar) in unstimulated (n = 23) and stimulated (n = 26) control, unstimulated (n = 24) and stimulated (n = 27) Y-27632-treated cells are 1 ± 0.03, 1.3 ± 0.02, 1.17 ± 0.03, and 1.22 ± 0.03, respectively. P values are as indicated.

directional transport of vesicles in polarized systems such as epithelial cells (Stow et al., 1998). Because RhoA signaling is involved in cell adhesion (Arthur et al., 2002), adhesion components may also be coupled to the spatial regulation of PRG containing-vesicles.

While myosin II regulates the localization of PRG, it may not be necessary for fMLP to activate RhoA, as suggested by the effect of inhibiting ROCK with Y-27632 (Fig. 4 B). We used Y-27632, rather than blebbistatin, to block fMLP-induced ROCK-dependent activation of myosin II (this avoids interference by blebbistatin fluorescence with RhoA FRET). In cells quasi-stably expressing the RhoA biosensor (Wong et al., 2006), inhibiting ROCK and therefore myosin II does not reduce RhoA activity (Fig. 4 B). Instead, ROCK-inhibited cells show elevated basal RhoA FRET compared with unstimulated controls and fMLP fails to further increase the level of active RhoA (Fig. 4 B). The RhoA FRET signal, like PRG-YFP in ROCK-inhibited cells, is highest around the nucleus, in contrast to the back localization in controls (Fig. 4 C; the nucleus is visible because it excludes the RhoA biosensor).

The findings that myosin II regulates PRG by spatially focusing its activity rather than by controlling its level of activity suggest a mechanism in which G12/13, PRG, RhoA, and myosin II cooperate to spatially self-confine and concentrate backness-promoting signals. In addition to G12/13 and myosin II, two other reported mechanisms may help confine PRG to the back and exclude it from the front: PRG's interaction with F-actin has been suggested to suppress its GEF activity (Banerjee and Wedegaertner, 2004), and PAK4, an effector of Cdc42, has been reported (Barac et al., 2004) to phosphorylate PRG and inhibit its activity.

Positive feedback loops for the front, involving PIP3, Rac, and protrusive actin, activate and reinforce one another to form and ensure a robust front (Wang et al., 2002; Weiner et al., 2002). Now we identify a mechanism in which backness components G12/13, PRG, RhoA, ROCK, myosin II, and actomyosin spatially consolidate and strengthen one another at the back. Together with the mutual exclusivity between front and back activities (Xu et al., 2003), these two divergent signaling pathways create distinct subcellular environments that favor the propagation of their own signals, thereby facilitating their segregation from one another during symmetry breaking.

PIP3 and microtubules are both reported to regulate backness (Niggli, 2003; Xu et al., 2005; Van Keymeulen et al., 2006), but our experiments so far do not allow us to draw firm inferences regarding the possible role of microtubules in regulating localization of PRG-YFP (see Online supplemental materials, available at http://www.jcb.org/cgi/content/full/jcb.200706167/DC1).

Materials and methods

Constructs and antibodies

Myc-tagged human PRG and its deletion mutants were gifts from Philip Wedegaertner (Thomas Jefferson University, Philadelphia, PA). C-terminally YFP-tagged human full-length and mutant PRG were generated by PCR using the myc-tagged constructs as templates and the resulting PCR fragments cloned into EcoRI and SalI sites in pEYFP-C1. The tetracycline-inducible construct was generated by inserting PRG-YFP into pTRE (Clontech Laboratories, Inc.). Myc-tagged rat PRG was a gift from Mandy Jackson (University of Edinburgh, Edinburgh, UK). The RhoA biosensor construct used for transient transfection was as described (Pertz et al., 2006). G12-DN and G13-DN constructs (residues 326–379 for Gα12, and residues 321–377 for Gα13) were as described (Sugimoto et al., 2003). CA mutants of Gα12 and Gα13 were obtained from Guthrie Institute (Sayre, PA). Lentiviral shRNA construct targeting human PRG was generated by cloning a 5′-tcaacgctgtgtcattatccaa-3′ sequence into pPRIME-CMV-GFP-FF3 according to the protocol for pPRIME (Stegmeier et al., 2005). This construct contained GFP for identification of shRNA expression. An empty pPRIME-CMV-GFP-FF3 vector that contained GFP and hairpin targeting firefly luciferase was used as a control. Rabbit polyclonal antibody against PRG was a gift from John Rothstein (The Johns Hopkins University, Baltimore, MD). Mouse monoclonal antibody against myosin light chain 2 phosphorylated at S19 (p-MLC2) was from Cell Signaling Technology. Antibodies against RhoA, and c-myc were from Santa Cruz Biotechnology, Inc. Blebbistatin and PIK-90 were gifts from Tim Mitchison (Harvard University, Boston, MA) and Kevan Shokat (University of California, San Francisco, San Francisco, CA), respectively. Y-27632 and nocodazole were from Calbiochem. Alexa350- and rhodamine-phalloidin were obtained from Molecular Probes. Human fibronectin was from BD Biosciences. Nocodazole, protease and phosphatase inhibitor cocktails and fMLP were from Sigma-Aldrich. Horseradish peroxidase–conjugated donkey anti–rabbit and anti–mouse IgG, FITC or rhodamine-conjugated anti–rabbit and anti–mouse IgG were from GE Healthcare.

Cell culture, transient transfection, and lentiviral expression

HL60 cells were cultivated, differentiated, and transiently transfected as previously described (Servant et al., 2000; Srinivasan et al., 2003); experiments were performed 3–4 h after transfection unless otherwise indicated. Quasi-stable expression of control and PRG shRNAs was accomplished by lentiviral transfection and infected cells were FAC sorted for GFP expression as described (Wong et al., 2006).

Microscopy

Live dHL60 cells on coverslips in 1.5% human albumin in mHBSS or fixed cells in PBS were imaged at room temperature using an inverted microscope (Eclipse TE2000-E; Nikon) equipped with a Photometrics CoolSnap HQ CCD camera (Roper Scientific) driven by MetaMorph software (MDS Analytical Technologies). Pictures shown were taken with a 40× NA1.30 oil S Fluor objective (Nikon). Fluorochromes used include YFP, CFP, RFP, rhodamine, Alexa350, Texas red, and FITC. Cells were tracked using MetaMorph software (MDS Analytical Technologies).

FRET analysis

Cells transiently transfected with the RhoA biosensor were stimulated with or without 100 nM fMLP for 3 min, fixed, and imaged as described (Wong et al., 2006). FRET data were processed and subjected to statistical analysis as described (Wong et al., 2006). Unless stated otherwise, values from at least 14 cells were used to assess mean FRET/CFP ratios for each condition. Each set of experiment was repeated at least three times.

Assay for particulate-associated RhoA

Procedure and analysis for this assay were as described (Van Keymeulen et al., 2006).

Actin and immunofluorescence staining

Procedures for actin staining and immunofluorescence have been described (Xu et al., 2003; Van Keymeulen et al., 2006).

Online supplemental material

Figure S1 shows that depletion of PRG causes migratory defects. Figure S2 shows how disrupted PDZRhoGEF function disrupts fMLP-induced polarity. Figure S3 shows background fluorescence of blebbistatin. Online supplemental material is available at http://www.jcb.org/cgi/content/full/jcb.200706167/DC1.

Similar results were observed in three independent experiments. **, $P \leq 0.05$. (C) Representative DIC, CFP, and FRET/CFP ratio images of control and Y-27632–treated cells. Ratio images were scaled relative to each other. Warm color = high value, cold color = low value. Different color of arrowheads marks different pseudopod. Bars = 10 μm.

We thank members of the Bourne lab, Philip Wedegaertner, Jayashree Banerjee, Orion Weiner, Keith Mostov, and Max Krummel for advice and useful comments on the manuscript.

This work was supported by National Institutes of Health (NIH) grant GM27800 (to H.R. Bourne). K. Wong and A. Van Keymeulen were postdoctoral fellows supported by the American Heart Association. K. Wong is now supported by NIH Grant GM27800.

Submitted: 22 June 2007
Accepted: 15 November 2007

References

Arthur, W.T., N.K. Noren, and K. Burridge. 2002. Regulation of Rho Family GTPases by Cell-Cell and Cell-Matrix Adhesion. *Biol. Res.* 35:239–246.

Banerjee, J., and P.B. Wedegaertner. 2004. Identification of a novel sequence in PDZ-RhoGEF that mediates interaction with the actin cytoskeleton. *Mol. Biol. Cell.* 15:1760–1775.

Barac, A., J. Basile, J. Vazquez-Prado, Y. Gao, Y. Zheng, and J.S. Gutkind. 2004. Direct interaction of p21-activated kinase 4 with PDZ-RhoGEF, a G protein-linked Rho guanine exchange factor. *J. Biol. Chem.* 279:6182–6189.

Basile, J.R., A. Barac, T. Zhu, K.L. Guan, and J.S. Gutkind. 2004. Class IV semaphorins promote angiogenesis by stimulating Rho-initiated pathways through plexin-B. *Cancer Res.* 64:5212–5224.

Driessens, M.H., C. Olivo, K. Nagata, M. Inagaki, and J.G. Collard. 2002. B plexins activate Rho through PDZ-RhoGEF. *FEBS Lett.* 529:168–172.

Francis, S.A., X. Shen, J.B. Young, P. Kaul, and D.J. Lerner. 2006. Rho GEF Lsc is required for normal polarization, migration, and adhesion of formyl-peptide-stimulated neutrophils. *Blood.* 107:1627–1635.

Fukata, M., M. Nakagawa, and K. Kaibuchi. 2003. Roles of Rho-family GTPases in cell polarisation and directional migration. *Curr. Opin. Cell Biol.* 15:590–597.

Fukuhara, S., C. Murga, M. Zohar, T. Igishi, and J.S. Gutkind. 1999. A novel PDZ domain containing guanine nucleotide exchange factor links heterotrimeric G proteins to Rho. *J. Biol. Chem.* 274:5868–5879.

Hannigan, M., L. Zhan, Z. Li, Y. Ai, D. Wu, and C.K. Huang. 2002. Neutrophils lacking phosphoinositide 3-kinase gamma show loss of directionality during N-formyl-Met-Leu-Phe-induced chemotaxis. *Proc. Natl. Acad. Sci. USA.* 99:3603–3608.

Hauert, A.B., S. Martinelli, C. Marone, and V. Niggli. 2002. Differentiated HL-60 cells are a valid model system for the analysis of human neutrophil migration and chemotaxis. *Int. J. Biochem. Cell Biol.* 34:838–854.

Hirsch, E., V.L. Katanaev, C. Garlanda, O. Azzolino, L. Pirola, L. Silengo, S. Sozzani, A. Mantovani, F. Altruda, and M.P. Wymann. 2000. Central role for G protein-coupled phosphoinositide 3-kinase gamma in inflammation. *Science.* 287:1049–1053.

Kunisaki, Y., A. Nishikimi, Y. Tanaka, R. Takii, M. Noda, A. Inayoshi, K. Watanabe, F. Sanematsu, T. Sasazuki, T. Sasaki, and Y. Fukui. 2006. DOCK2 is a Rac activator that regulates motility and polarity during neutrophil chemotaxis. *J. Cell Biol.* 174:647–652.

Li, Z., H. Jiang, W. Xie, Z. Zhang, A.V. Smrcka, and D. Wu. 2000. Roles of PLC-beta2 and -beta3 and PI3Kgamma in chemoattractant-mediated signal transduction. *Science.* 287:1046–1049.

Li, Z., M. Hannigan, Z. Mo, B. Liu, W. Lu, Y. Wu, A.V. Smrcka, G. Wu, L. Li, and M. Liu. 2003. Directional sensing requires G[beta][gamma]-mediated PAK1 and PIX[alpha]-dependent activation of Cdc42. *Cell.* 114:215–227.

Longhurst, D.M., M. Watanabe, J.D. Rothstein, and M. Jackson. 2006. Interaction of PDZRhoGEF with microtubule-associated protein 1 light chains: link between microtubules, actin cytoskeleton, and neuronal polarity. *J. Biol. Chem.* 281:12030–12040.

Narumiya, S., T. Ishizaki, and M. Uehata. 2000. Use and properties of ROCK-specific inhibitor Y-27632. *Methods Enzymol.* 325:273–284.

Niggli, V. 2000. A membrane-permeant ester of phosphatidylinositol 3,4, 5-trisphosphate (PIP(3)) is an activator of human neutrophil migration. *FEBS Lett.* 473:217–221.

Niggli, V. 2003. Microtubule-disruption-induced and chemotactic-peptide-induced migration of human neutrophils: implications for differential sets of signalling pathways. *J. Cell Sci.* 116:813–822.

Panizzi, J.R., J.R. Jessen, I.A. Drummond, and L. Solnica-Krezel. 2007. New functions for a vertebrate Rho guanine nucleotide exchange factor in ciliated epithelia. *Development.* 134:921–931.

Pertz, O., L. Hodgson, R.L. Klemke, and K.M. Hahn. 2006. Spatiotemporal dynamics of RhoA activity in migrating cells. *Nature.* 440:1069–1072.

Raftopoulou, M., and A. Hall. 2004. Cell migration: Rho GTPases lead the way. *Dev. Biol.* 265:23–32.

Rogers, S.L., U. Wiedemann, U. Hacker, C. Turck, and R.D. Vale. 2004. *Drosophila* RhoGEF2 associates with microtubule plus ends in an EB1-dependent manner. *Curr. Biol.* 14:1827–1833.

Rossman, K.L., C.J. Der, and J. Sondek. 2005. GEF means go: turning on Rho GTPases with guanine nucleotide-exchange factors. *Nat. Rev. Mol. Cell Biol.* 6:167–180.

Rumenapp, U., A. Blomquist, G. Schworer, H. Schablowski, A. Psoma, and K.H. Jakobs. 1999. Rho-specific binding and guanine nucleotide exchange catalysis by KIAA0380, a dbl family member. *FEBS Lett.* 459:313–318.

Servant, G., O.D. Weiner, P. Herzmark, T. Balla, J.W. Sedat, and H.R. Bourne. 2000. Polarization of chemoattractant receptor signaling during neutrophil chemotaxis. *Science*. 287:1037–1040.

Shields, J.M., and W.S. Haston. 1985. Behaviour of neutrophil leucocytes in uniform concentrations of chemotactic factors: contraction waves, cell polarity and persistence. *J. Cell Sci.* 74:75–93.

Srinivasan, S., F. Wang, S. Glavas, A. Ott, F. Hofmann, K. Aktories, D. Kalman, and H.R. Bourne. 2003. Rac and Cdc42 play distinct roles in regulating PI(3,4,5)P3 and polarity during neutrophil chemotaxis. *J. Cell Biol.* 160:375–385.

Stegmeier, F., G. Hu, R.J. Rickles, G.J. Hannon, and S.J. Elledge. 2005. A lentiviral microRNA-based system for single-copy polymerase II-regulated RNA interference in mammalian cells. *Proc. Natl. Acad. Sci. USA.* 102:13212–13217.

Stow, J.L., K.R. Fath, and D.R. Burgess. 1998. Budding roles for myosin II on the Golgi. *Trends Cell Biol*. 8:138–141.

Sugimoto, N., N. Takuwa, H. Okamoto, S. Sakurada, and Y. Takuwa. 2003. Inhibitory and stimulatory regulation of Rac and cell motility by the G12/13-Rho and Gi pathways integrated downstream of a single G protein-coupled sphingosine-1-phosphate receptor isoform. *Mol. Cell. Biol.* 23:1534–1545.

Swiercz, J.M., R. Kuner, J. Behrens, and S. Offermanns. 2002. Plexin-B1 directly interacts with PDZ-RhoGEF/LARG to regulate RhoA and growth cone morphology. *Neuron.* 35:51–63.

Van Keymeulen, A., K. Wong, Z.A. Knight, C. Govaerts, K.M. Hahn, K.M. Shokat, and H.R. Bourne. 2006. To stabilize neutrophil polarity, PIP3 and Cdc42 augment RhoA activity at the back as well as signals at the front. *J. Cell Biol.* 174:437–445.

Wang, F., P. Herzmark, O.D. Weiner, S. Srinivasan, G. Servant, and H.R. Bourne. 2002. Lipid products of PI(3)Ks maintain persistent cell polarity and directed motility in neutrophils. *Nat. Cell Biol*. 4:513–518.

Weiner, O.D., P.O. Neilsen, G.D. Prestwich, M.W. Kirschner, L.C. Cantley, and H.R. Bourne. 2002. A PtdInsP3- and Rho GTPase-mediated positive feedback loop regulates neutrophil polarity. *Nat. Cell Biol.* 4:509–513.

Wong, K., O. Pertz, K. Hahn, and H. Bourne. 2006. Neutrophil polarization: spatiotemporal dynamics of RhoA activity support a self-organizing mechanism. *Proc. Natl. Acad. Sci. USA.* 103:3639–3644.

Xu, J., F. Wang, A. Van Keymeulen, P. Herzmark, A. Straight, K. Kelly, Y. Takuwa, N. Sugimoto, T. Mitchison, and H.R. Bourne. 2003. Divergent signals and cytoskeletal assemblies regulate self-organizing polarity in neutrophils. *Cell.* 114:201–214.

Xu, J., F. Wang, A. Van Keymeulen, M. Rentel, and H.R. Bourne. 2005. Neutrophil microtubules suppress polarity and enhance directional migration. *Proc. Natl. Acad. Sci. USA.* 102:6884–6889.